

Reflection–absorption infrared investigation of hydrogenated silicon oxide generated by the thermal decomposition of $\text{H}_8\text{Si}_8\text{O}_{12}$ clusters

K. T. Nicholson, K. Z. Zhang, and M. M. Banaszak Holl^{a)}
Department of Chemistry, University of Michigan, Ann Arbor, Michigan 48109-1055

F. R. McFeely
IBM T. J. Watson Laboratory, Yorktown Heights, New York 10598

(Received 9 October 2001; accepted for publication 22 February 2002)

Reflection–absorption infrared spectroscopy has been employed to observe Si–H bonds within a model, ultrathin silicon oxide. Upon heating a monolayer of $\text{H}_8\text{Si}_8\text{O}_{12}/\text{Si}(100)-2\times 1$ to 700 °C, Si–H bonds as a part of HSiO_3 entities are still detected within the oxide layer after cooling. These fragments appear to be stable to temperatures of at least 850 °C. Reversible hydrogen/deuterium exchange for these entities is also directly observed. © 2002 American Institute of Physics.

[DOI: 10.1063/1.1469662]

INTRODUCTION

The atomic structure and reactivity of the Si/SiO₂ interface have become increasingly important to the microelectronics industry as device size continues to shrink.^{1,2} Electrical functionality will eventually be dominated by the physical and chemical nature of the solid/solid interfaces that make up the devices. Si–H bond breaking and formation in and near the Si/SiO₂ interface during operation has been suggested to lead to device breakdown and failure.^{3–10} This phenomenon is typically correlated with thermal and/or electrical stress on the oxide. After annealing thin amorphous silicon oxide ($\alpha\text{-SiO}_x$) layers at temperature >550 °C, electron paramagnetic resonance (EPR) studies have illustrated that interface states (such as three coordinate silicon dangling bonds) form upon the breaking of Si–H bonds near the Si/SiO₂ interface.^{11–13} Some of these states can be passivated or depassivated by introducing atomic hydrogen.^{7,9,11} In a similar way, hydrogen atoms have been observed to enter ultrathin oxide films at 23 °C and escape upon annealing at 670 °C by x-ray photoelectron spectroscopy (XPS).¹⁴

Ultrathin oxides (<1 nm thick) on Si(100)-2×1 with various hydrogen contents can be created using a variety of techniques. The most common method involves heating a clean Si sample to 700 °C in the presence of oxygen followed by a thermal anneal in the presence of hydrogen gas.¹⁵ This method limits the amount of hydrogen in the film while insuring many of the paramagnetic interface states are passivated. To better understand the growth mechanism and chemical structure of interfacial SiO₂, other precursor deposition methods have been previously reported in the literature as well. For example, Weldon and co-workers have extensively studied the stepwise formation of silicon oxide using water.^{16–18} Based upon infrared and XPS experiments, water has been proposed to dissociatively adsorb across a Si(100)-2×1 row at room temperature. Upon heating the single layer, the $\nu(\text{Si-H})$ infrared adsorption frequency shifts from

~2050 to 2250 cm^{-1} which is consistent with the conversion to new, more thermally stable, HSiO_3 entities at this model Si/SiO₂ interface. Upon further heating to 650 °C, the HSiO_3 entities are no longer detected and an infrared signature consistent with the presence of silicon epoxide structures is observed.

Hydridosilsesquioxane clusters, $(\text{HSiO}_{1.5})_n$, an oxide precursor solely composed of HSiO_3 entities, also chemisorb to Si(100)-2×1 to form ultrathin layers.^{19–21} The well-defined thin oxide film formed in this manner is made up of clusters containing seven HSiO_3 fragments. This system has been characterized using XPS,^{19,20,22–25} reflection–absorption infrared spectroscopy (RAIRS),^{26,27} and scanning tunneling microscopy (STM).²⁸ It is particularly well suited for studying the spectroscopic changes associated with thermal stress or the reaction with hydrogen radicals. Upon heating the precursor derived oxide layer to >300 °C, the photoemission characteristics of an ultrathin, thermally grown oxide are observed in both the Si 2*p* core-level spectra as well as in the valence band (Fig. 1). Unfortunately, XPS alone cannot adequately describe the chemical structure and stability of the Si–H bonds in the cluster-generated oxide film as a function of the temperature. In this article, we report a reflection–absorption infrared spectroscopy investigation of this model system to garner a better understanding of the chemical reactivity of HSiO_3 in model device interfaces. First, the thermal stability of the HSiO_3 fragment will be examined. After heating to ~700 °C, ~15% of the original entities appear to be broken based on the integrated intensity of the $\nu(\text{Si-H})$ feature. However, many of the Si–H bonds remain in the <1 nm thick oxide layer until it is heated to ~850 °C, the temperature at which the oxide layer begins to evaporate from the surface. Second, the hydrogen/deuterium exchange characteristics of the Si–H bonds will be investigated. In fact, Si–H bonds within the stable HSiO_3 entities can also be substituted for Si–D bonds upon exposure to deuterium atoms at 25 °C. The isotopic exchange appears to be completely reversible upon the introduction of hydrogen atoms.

^{a)}Electronic mail: mbanasza@umich.edu

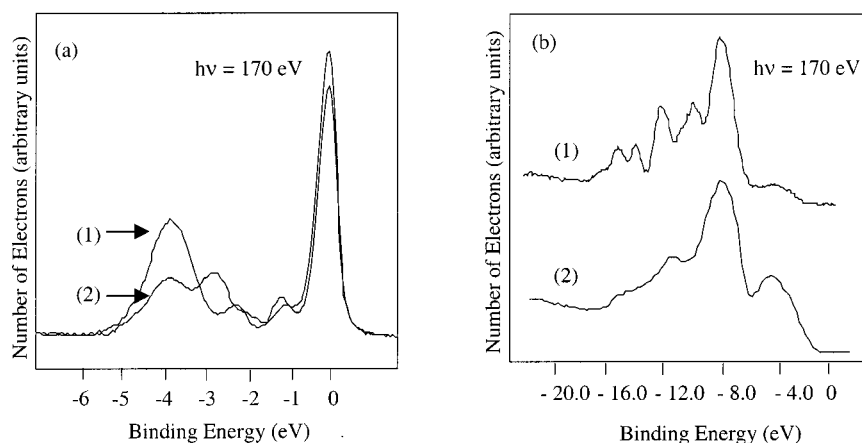


FIG. 1. (a) (1) Soft x-ray photoemission spectra of the Si 2*p* core levels after chemisorption of $H_8Si_8O_{12}$ onto Si(100)-2 \times 1. Binding energies (BE) are reported vs bulk silicon (BE = -99 eV). (2) Si 2*p* core levels after heating (1) to 590 °C. (b) (1) Soft x-ray photoemission spectra of the valence band region (BE = 0 to -22 eV) after chemisorption of $H_8Si_8O_{12}$ onto Si(100)-2 \times 1. Valence band region of the $H_8Si_8O_{12}$ /Si layer after heating (1) to 590 °C.

EXPERIMENT

Reflection-absorption infrared spectroscopy was employed to investigate the reactivity of Si-H bonds within ultrathin silicon oxide films. RAIRS is a reflection based, nondestructive, surface analytical technique that has the capability to scan a larger portion of the infrared region (50–4000 cm^{-1}) than other surface infrared techniques such as multiple internal reflectance (MIR) and attenuated total reflectance.^{29,30} The very intense ν_{as} (Si-O-Si) vibrational mode (950–1300 cm^{-1}) can be detected by RAIRS; therefore, the stability of Si-H bonds can also be discussed in terms of changes within the oxide itself. The RAIRS experiments were performed in an UHV chamber (base pressure 5×10^{-10} Torr) that is described in detail elsewhere.³¹ Each scan set consisted of 128 scans at 8 cm^{-1} resolution.

The ultrathin (<1 nm thick) silicon oxide films were formed on Si(100)-2 \times 1 using a precursor based method. The Si(100)-2 \times 1 samples used for all of the RAIRS experiments included a CoSi mirror to increase the reflectivity. The preparation of these samples is described in detail elsewhere.^{31–33} Before introduction into the UHV chamber the samples were cleaned by standard RCA methods. The sample was degassed for ~ 3 h in UHV at ~ 300 °C and allowed to cool before being transferred into the RAIRS chamber and aligned. The native, wet-chemical oxide was removed by heating the sample to ~ 1050 °C for ~ 30 s. The sample was allowed to cool for ~ 15 min before a background scan set was collected. At this point, ~ 7 L (1 L = 1.0×10^{-6} Torr s) of $H_8Si_8O_{12}$ clusters was introduced into the chamber at a dosing pressure of 5.0×10^{-8} torr. Hydridosilsesquioxane clusters, such as $H_8Si_8O_{12}$,^{34–37} are convenient precursors for hydrogen containing ultrathin silicon oxide films because they are volatile and form a monolayer on Si(100)-2 \times 1 at ~ 22 °C.^{19,31,38} The clusters also have ν (Si-H) and δ (H-SiO₃) vibrational modes with a fairly intense, very distinct infrared signature [Fig. 2(a)].

Ultrathin (<1 nm thick) *a*-SiO₂ results when the monolayer of $H_8Si_8O_{12}$ /Si(100)-2 \times 1 is heated to >300 °C (Fig. 1).³⁹ The seven specific cluster features in the valence band region disappear upon heating the layer, yielding an amorphous oxide layer. In fact, both the valence band region and the Si 2*p* core levels become identical to those observed for

the thermal oxidation of Si(100)-2 \times 1 by O₂ (Fig. 1).^{1,40} Therefore, the clusters provide a unique precursor for the generation of hydrogenated *a*-SiO₂ films that specifically contain HSiO₃ entities amenable to a RAIRS investigation.

XPS spectra, specifically of the Si 2*p* core levels and valence band region, were collected at the National Synchrotron Light Source, Brookhaven National Laboratories, at beamline U8B using an incident photon energy of 170 eV. The UHV apparatus and detector used are described elsewhere.³⁹ For this experiment, the Si sample was flashed, dosed, and heated in a separate vacuum chamber (base pressure 2×10^{-10} Torr) and then transferred to an XPS analysis chamber (base pressure 2×10^{-10} Torr). The Si 2*p*_{1/2} core level was stripped using MATLAB 4.2C. This program was also employed for curve fitting and peak area analysis. A conventional XPS spectrometer with a Mg *K* α source was employed to collect O 1*s* core-level spectra.³⁹

Exposure of hydrogen and deuterium atoms to the model silicon oxides was accomplished by introducing H₂ or D₂ to a heated tungsten filament (~ 1400 °C) situated ~ 8 cm from

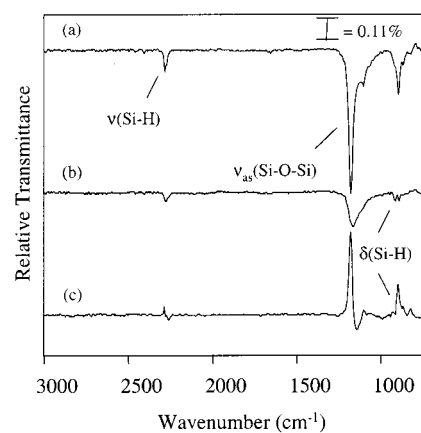


FIG. 2. (a) Reflection-absorption infrared (750–3000 cm^{-1}) spectrum of a chemisorbed layer of $H_8Si_8O_{12}$ on Si(100)-2 \times 1. (b) Reflection-absorption infrared spectrum of the $H_8Si_8O_{12}$ /Si layer after the sample was heated to ~ 700 °C for 5 s. Both (a) and (b) consist of three scan sets referenced to a clean Si background. (c) Overall change in the chemisorbed layer after heating. These data are representative of three scan sets referenced to a chemisorbed layer of $H_8Si_8O_{12}$ /Si.

the sample. The specific exposure times for the hydrogen and deuterium radical experiments may be found in the appropriate figure captions.

RESULTS AND DISCUSSION

The formation of a model, hydrogen-containing, <1 nm thick oxide was just described. A monolayer of $\text{H}_8\text{Si}_8\text{O}_{12}$ on $\text{Si}(100)\text{-}2\times 1$ has the infrared signature illustrated in Fig. 2(a). After heating the layer to $\sim 700^\circ\text{C}$ for 5 s, the oxide layer changes significantly [Fig. 2(b)]. This spectrum, referenced to a clean $\text{Si}(100)\text{-}2\times 1$ surface, was taken after the sample was allowed to cool for ~ 15 min. The intensity of $\nu(\text{H-SiO}_3)$ at 2271 cm^{-1} decreases by $\sim 15\%$ [Fig. 2(b)]. The $\delta(\text{HSiO}_3)$ features at 858 , 888 , and 905 cm^{-1} of the initial cluster layer are more significantly altered [Fig. 2(b)]. For example, the peak at 858 cm^{-1} is no longer observed after heating. Only two small $\delta(\text{H-SiO}_3)$ features, of nearly identical intensity, are detected at 905 and 888 cm^{-1} [Fig. 2(b)]. Changes are also detected for the $\nu_{as}(\text{Si-O-Si})$ and $\nu_s(\text{Si-O-Si})$ regions as well. Specifically, the frequency of the most intense $\nu_{as}(\text{Si-O-Si})$ feature at 1177 cm^{-1} for the initial monolayer [Fig. 2(a)] shifts to 1154 cm^{-1} after heating whereas the $\nu_s(\text{Si-O-Si})$ peak at 820 cm^{-1} disappears [Fig. 2(b)]. An increase in intensity in the $1100\text{--}1140\text{ cm}^{-1}$ region is also detected while a prominent negative peak is observed at 1181 cm^{-1} [Fig. 2(c)]. A shoulder, clearly resolved in Fig. 2(a) to be centered at $\sim 1090\text{ cm}^{-1}$, is hardly distinguishable from the major peak after heating [Fig. 2(b)]. No further changes are detected after heating the sample for three additional 5 s intervals at 700°C .

Although significant diminutions in RAIRS intensity are detected for all of the cluster vibrational modes [Fig. 2(c)], the total integrated intensities of the O $1s$ and Si $2p$ core levels do not change after heating the initial monolayer to 700°C . As previously mentioned, the Si $2p$ core-level and valence band data for the heated cluster layer are identical to those observed for an ultrathin, thermally grown, annealed oxide using O_2 (Fig. 1). The net integrated intensity of all the core levels measured remains constant in this temperature regime.

The diminutions in RAIRS intensity at 2271 , 905 , and 888 cm^{-1} suggest the Si-H bonds of some of the HSiO_3 vertices have broken and a hydrogen-containing Si/SiO₂ interface has formed. At 700°C , these fragments may have reacted with unpassivated atoms of the silicon surface. Alternatively, based on the RAIRS data alone, the original Si-H bonds may have become reoriented in a way that reduced the IR signal intensity. The gross intensity changes in the $\delta(\text{Si-H})$ region are consistent with the formation of an ultrathin amorphous oxide layer upon heating [Fig. 2(b)]. The features of the heated oxide at 2271 , 905 , and 886 cm^{-1} suggest the remaining Si-H bonds still consist of HSiO_3 fragments [Fig. 2(b)]. Since the adsorption frequencies are identical, it is possible that a portion of the original cluster vertices remain intact after heating, stabilized by the neighboring oxide through reaction with the bulk silicon surface. Hydrogen bonding and/or other intermolecular forces within the oxide have been proposed to increase the stability of

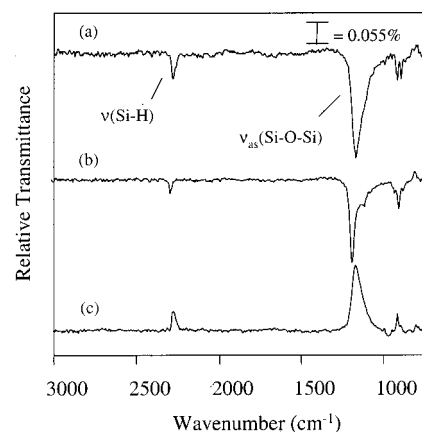


FIG. 3. (a) RAIRS ($750\text{--}3000\text{ cm}^{-1}$) spectrum of a $\text{H}_8\text{Si}_8\text{O}_{12}/\text{Si}$ layer after the sample is heated to $\sim 700^\circ\text{C}$ for 5 s. (b) RAIRS spectrum of the $\text{H}_8\text{Si}_8\text{O}_{12}/\text{Si}$ -based oxide layer after being further heated to 700 and 850°C in 5 s intervals. Both (a) and (b) are illustrative of three scan sets referenced to a clean Si background. (c) Difference spectrum that illustrates the changes within the oxide layer after being heated to 700 and 850°C in 5 s intervals. This spectrum represents three scan sets referenced to a $\text{H}_8\text{Si}_8\text{O}_{12}/\text{Si}$ -based, thermally grown oxide layer after one 5 s anneal at 700°C [shown in (a)].

Si-H bonds.¹¹ While most of the hydrogen would be expected to escape, a few H atoms may remain trapped in the oxide. As the sample cools, the trapped H atoms could react with unpassivated Si atoms and form new Si-H bonds. Regardless of the mechanism, Si-H bonds are still present in the cooled, ultrathin oxide until the film is heated to $\sim 850^\circ\text{C}$ (*vide infra*), the temperature at which the oxide layer evaporates, as monitored by RAIRS (Fig. 3) as well as by the Si $2p$ and O $1s$ core levels.

Structural changes within the oxide also accompany the changes in the $\nu(\text{Si-H})$ and $\delta(\text{Si-H})$ regions. Features within the $\nu_{as}(\text{Si-O-Si})$ region at lower frequency suggest the formation of new Si-O bonds by a surface silicon atom generating low oxidation state Si moieties during the decomposition of HSiO_3 fragments. However, the most intense feature at 1154 cm^{-1} , shifted only 23 cm^{-1} from its position for the original cluster monolayer, implies there are still many Si-SiO₃ pieces present within the cooled oxide [Fig. 2(b)]. Since the characteristic frequency range of SiO₂ overlaps Si-SiO₃ and HSiO_3 , especially at ~ 1 nm thickness, the formation of some amorphous SiO₂ (without the addition of oxygen) upon heating also cannot be disregarded.¹⁵

These RAIRS data may also be interpreted in conjunction with previously published Si $2p$ core-level data for the formation of an ultrathin oxide using this precursor-based method.^{39,41} Soft x-ray photoemission spectra of the chemisorption of $\text{H}_8\text{Si}_8\text{O}_{12}$ onto $\text{Si}(100)\text{-}2\times 1$ followed by subsequent heating at 590°C for ~ 2 min are illustrated in Fig. 1. The total intensity of the feature derived from H-SiO₃ cluster fragments, centered at $\sim -3.6\text{ eV}$, loses over 50% of its original intensity after heating.^{19,42-45} A new feature, centered at $\sim -2.7\text{ eV}$, is also observed that is $\sim 60\%$ as intense as the broad feature at -3.6 eV . The ratio of oxidized silicon to bulk silicon remains constant and the total oxygen (measured by the O $1s$ core level) is the same before and after heating. However, analysis of volatile products by mass spectrometry shows hydrogen evolution at 590°C that is concurrent with the appearance of the new feature at -2.7

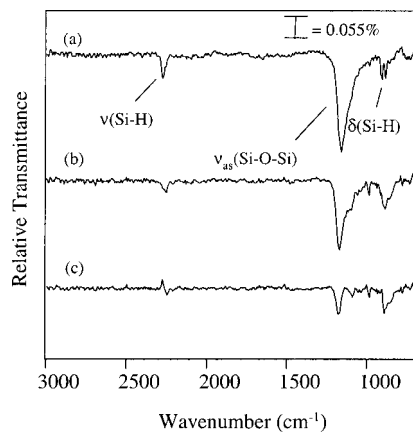


FIG. 4. (a) RAIRS (750–3000 cm^{-1}) spectrum of a $\text{H}_8\text{Si}_8\text{O}_{12}/\text{Si}$ layer after the sample is heated to $\sim 700^\circ\text{C}$ for 5 s. This spectrum illustrates three scan sets referenced to a clean Si background. (b) RAIRS spectrum of the $\text{H}_8\text{Si}_8\text{O}_{12}/\text{Si}$ -based oxide layer (a) after being exposed to hydrogen (1.0×10^{-5} Torr) in the presence of a tungsten filament (1400°C) for 5 min. These data are representative of five scan sets referenced to a clean Si background. (c) Overall change in the oxide layer after being exposed to hydrogen atoms. This spectrum represents five scan sets referenced to a $\text{H}_8\text{Si}_8\text{O}_{12}/\text{Si}$ -based, thermally grown oxide layer [shown in (a)].

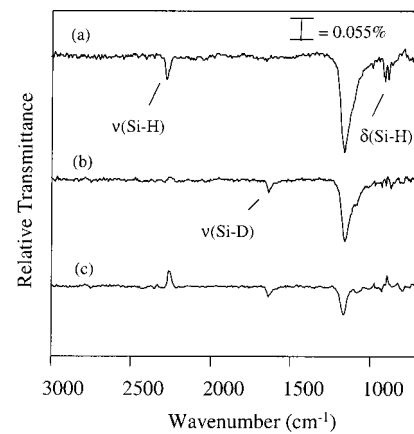


FIG. 5. (a) RAIRS (750–3000 cm^{-1}) spectrum of a $\text{H}_8\text{Si}_8\text{O}_{12}/\text{Si}$ layer after the sample is heated to $\sim 700^\circ\text{C}$ for 5 s. This spectrum illustrates three scan sets referenced to a clean Si background. (b) RAIRS spectrum of a $\text{H}_8\text{Si}_8\text{O}_{12}/\text{Si}$ -based oxide layer (a) after being exposed to deuterium (1.0×10^{-5} Torr) in the presence of a tungsten filament (1400°C) for 5 min. This spectrum represents five scan sets referenced to a clean Si background. (c) Overall change in the oxide layer after being exposed to deuterium atoms. These data are representative of five scan sets referenced to a $\text{H}_8\text{Si}_8\text{O}_{12}/\text{Si}$ -based, thermally grown oxide layer [shown in (a)].

eV. Recall, the Si $2p$ core levels and the valence band of the heated $\text{H}_8\text{Si}_8\text{O}_{12}$ -based oxide are similar to those observed for ultrathin, thermally grown, O_2 -based oxide XPS data collected at $500\text{--}640^\circ\text{C}$ (Fig. 1).³⁹ Heating for additional time yielded no significant changes in the x-ray photoelectron spectra at these temperatures.

These XPS observations are consistent with the previously discussed RAIRS data. The new photoemission feature at -2.7 eV that is observed upon heating combined with a $>50\%$ intensity loss in the -3.6 eV peak suggests that some of the Si–H bonds within the HSiO_3 entities are broken. Further evidence of this stems from the observation of H_2 by mass spectrometry that is consistent with the recombination of H atoms, presumably from the scission of Si–H bonds. However, the RAIRS data indicate many of the Si–H bonds remain in the film simply by observation of the $\nu(\text{Si-H})$ feature at 2271 cm^{-1} (Fig. 2). The intensity of the feature has only decreased by $\sim 15\%$ upon heating in comparison to the original layer of $\text{H}_8\text{Si}_8\text{O}_{12}$ on silicon. A very broadened $\nu_{as}(\text{Si-O-Si})$ feature is detected by IR, consistent with the presence of the amorphous silicon oxide layer that the Si $2p$ core level and valence band spectra also predict. This layer, however, contains substantially more hydrogen than the oxides that are thermally grown using O_2 and annealed in H_2 .

No additional changes are detected in the RAIRS data or O $1s$ core levels upon subsequent heating at ~ 700 , 750 , and 800°C in 5 s intervals. These observations further indicate silicon–hydrogen bonds are very robust in HSiO_3 entities, consistent with the Guerevich *et al.* study of impurity evolution in wet chemical oxides.⁴⁶ However, upon heating to 850°C , the integrated area of the O $1s$ core levels decreases by $\sim 40\%$. Upon subsequent heating at 850°C for 5–10 s, the rest of the oxide is removed and clean silicon remains.

Hydrogen atom exposure to the previously heated (700°C) silicon oxide film [Fig. 4(a)] does not reverse the temperature induced changes in the $\text{H}_8\text{Si}_8\text{O}_{12}/\text{Si}(100)\text{-}2\times 1$

layer (Fig. 1). Upon exposure, the frequency of the $\nu(\text{Si-H})$ feature shifts from 2274 to 2265 cm^{-1} and decreases in intensity. Oddly, $\delta(\text{Si-H})$ peaks have a higher integrated intensity [Figs. 4(b) and 4(c)] after the hydrogen atoms are introduced. The frequency of the most intense $\nu_{as}(\text{Si-O-Si})$ feature at 1154 cm^{-1} also shifts to 1158 cm^{-1} with a small change in intensity [Fig. 4(c)]. No difference in the O $1s$ core levels is observed. It appears the incoming hydrogen atoms exchange with already present Si–H bonds and induce another chemical change within the oxide that leads to the $\nu(\text{Si-H})$ frequency shift. The differences in intensity likely result from a net loss of hydrogen within the film and/or reorientation of the new, exchanged Si–H bonds (Fig. 4). Regardless, the exposure of hydrogen atoms does not return the sample to the original $\text{H}_8\text{Si}_8\text{O}_{12}/\text{Si}(100)\text{-}2\times 1$ layer [Fig. 2(a)]. An amorphous, hydrogen-containing, ultrathin oxide still remains.

Hydrogen/deuterium atom exchange is also observed for these ultrathin oxides. Upon exposure of deuterium atoms, the Si–H bonds become Si–D bonds with 100% conversion [Fig. 5(a)]. Note the appearance of $\nu(\text{Si-D})$ at 1645 cm^{-1} as $\nu(\text{Si-H})$ at 2274 cm^{-1} and $\delta(\text{Si-H})$ at 888 and 905 cm^{-1} , respectively, vanish. $\delta(\text{Si-D})$ is expected between 710 and 620 cm^{-1} and is out of the range for this experimental setup. This observation is consistent with some of the work of Lyding *et al.* in which D atoms were substituted for H atoms in the thermal annealing processing of model metal–oxide–semiconductor (MOS) devices.^{47,48} The exchange reaction is completely reversible upon the introduction of hydrogen atoms to the deuterated sample [Fig. 6(b)]. Note the reappearance of the Si–H infrared features at 2265 , 888 , and 905 cm^{-1} , similar to in the previously discussed hydrogen atom exposed, $\text{H}_8\text{Si}_8\text{O}_{12}$ -based model oxides (Fig. 4). The peak at 1645 cm^{-1} , indicative of Si–D bonds, is no longer detected.

In conclusion, Si–H bonds are directly observed by RAIRS within model, ultrathin silicon oxide film after an-

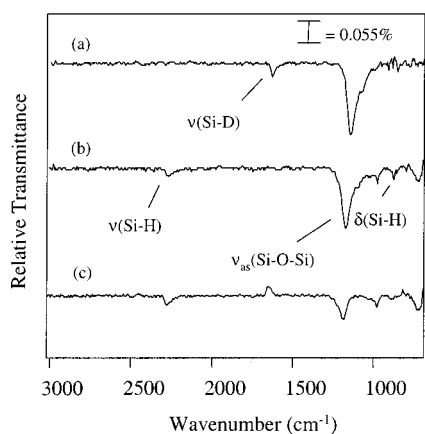


FIG. 6. (a) RAIRS (750–3000 cm^{-1}) spectrum of a $\text{H}_8\text{Si}_8\text{O}_{12}/\text{Si}$ -based oxide layer (a) after being exposed to deuterium (1.0×10^{-5} Torr) in the presence of a tungsten filament (1400 $^\circ\text{C}$) for 5 min. This spectrum illustrates five scan sets referenced to a clean Si background. (b) RAIRS spectrum of a deuterium exposed $\text{H}_8\text{Si}_8\text{O}_{12}/\text{Si}$ -based oxide layer (a) after being dosed with hydrogen (1.0×10^{-5} Torr) in the presence of a tungsten filament (1400 $^\circ\text{C}$). This spectrum represents five scan sets referenced to a clean Si background. (c) Overall change in the oxide layer (a) after being exposed to hydrogen atoms. This spectrum represents five scan sets referenced to a $\text{H}_8\text{Si}_8\text{O}_{12}/\text{Si}$ -based, thermally grown oxide layer previously exposed to deuterium atoms [shown in (a)].

nealing at temperatures >650 $^\circ\text{C}$. Although some of the initial HSiO_3 entities may decompose upon heating and form a silicon oxide with photoemission characteristics similar to that of the thermally grown oxide on $\text{Si}(100)\text{-}2 \times 1$, this study indicates that some Si–H bonds, specifically those within intact HSiO_3 entities, are quite stable to thermal stress. The remaining Si–H bonds are observed until the model oxide layer evaporates at ~ 850 $^\circ\text{C}$. However, the possibility that all of the initial HSiO_3 fragments are broken while the oxide is heated cannot immediately be disregarded. If this is indeed the case, significant atomic hydrogen must remain trapped within the <1 nm thick oxide and form new, RAIRS observable Si–H bonds as the sample cools.

Infrared and XPS characterizations of model, precursor-based, <1 nm thick, amorphous silicon oxide were employed to provide insight into the nature of one potential hydrogen-containing structure, HSiO_3 , that may be present in device quality oxides. This study has illustrated that HSiO_3 entities are quite stable to heat within this model oxide, consistent with the findings of Gurevich *et al.* for wet-chemical oxides.⁴⁶ Furthermore, reversible, isotopic substitution reactions can be directly observed by RAIRS upon exposure to hydrogen and deuterium atoms in concordance with the substitution reactions proposed by Lyding *et al.* in model MOS devices.^{47,48}

ACKNOWLEDGMENTS

The authors would like to acknowledge the National Science Foundation (DMR No. 0093641) for financial support of this research. The high-resolution photoemission experiments were completed at Brookhaven National Laboratory, National Synchrotron Light Source, at beamline U8b. One of

the authors (M.M.B.H.) appreciates support by an Alfred P. Sloan fellowship (1999–2002). The authors also thank Mehmet Dokmeci for slicing the specially prepared silicon samples used in the RAIRS experiments.

- ¹ *The Physics and Technology of Amorphous SiO₂*, edited by R. A. B. Devine (Plenum, New York, 1988).
- ² *The Physics and Chemistry of SiO₂ and the Si–SiO₂ Interface*, edited by C. R. Helms and B. E. Deal (Plenum, New York, 1993), Vol. 2.
- ³ D. L. Griscom, *J. Electron. Mater.* **21**, 762 (1992).
- ⁴ J. F. Conley and P. M. Lanahan, *IEEE Trans. Nucl. Sci.* **40**, 1335 (1993).
- ⁵ H. Ogawa, N. Terada, K. Sugiyama, K. Moriki, M. Noriyuki, T. Aoyama, R. Sugino, T. Ito, and T. Hattori, *Appl. Surf. Sci.* **56–58**, 836 (1992).
- ⁶ H. Ogawa and T. Hattori, *Appl. Phys. Lett.* **61**, 577 (1992).
- ⁷ E. Cartier, J. H. Stathis, and D. A. Buchanan, *Appl. Phys. Lett.* **63**, 1510 (1993).
- ⁸ K. D. Dobbs and D. J. Doren, *J. Am. Chem. Soc.* **115**, 3731 (1993).
- ⁹ J. H. Stathis and E. Cartier, *Phys. Rev. Lett.* **72**, 2745 (1994).
- ¹⁰ H. Ikeda, K. Hotta, S. Furuta, S. Zaima, and Y. Yasuda, *Appl. Surf. Sci.* **104–105**, 354 (1996).
- ¹¹ A. G. Revesz, *J. Electrochem. Soc.* **126**, 122 (1979).
- ¹² A. Stesmans and G. Van Gorp, *Appl. Phys. Lett.* **57**, 2663 (1990).
- ¹³ K. L. Brower and S. M. Myers, *Appl. Phys. Lett.* **57**, 162 (1990).
- ¹⁴ S. Lee, M. M. Banaszak Holl, W. H. Hung, and F. R. McFeely, *Appl. Phys. Lett.* **68**, 1081 (1996).
- ¹⁵ F. J. Himpsel, G. Hollinger, F. R. McFeely, A. Taleb-Ibrahimi, and J. A. Yarmoff, *Phys. Rev. B* **38**, 6084 (1988).
- ¹⁶ B. B. Stefanov, A. B. Gurevich, M. K. Weldon, K. Raghavachari, and Y. J. Chabal, *Phys. Rev. Lett.* **81**, 3908 (1998).
- ¹⁷ M. K. Weldon, K. T. Queeney, A. B. Gurevich, B. B. Stefanov, Y. J. Chabal, and K. Raghavachari, *J. Chem. Phys.* **113**, 2440 (2000).
- ¹⁸ M. K. Weldon, B. B. Stefanov, K. Raghavachari, and Y. J. Chabal, *Phys. Rev. Lett.* **79**, 2851 (1997).
- ¹⁹ M. M. Banaszak Holl and F. R. McFeely, *Phys. Rev. Lett.* **71**, 2441 (1993).
- ²⁰ S. Lee, S. M. M. M. Banaszak Holl, and F. R. McFeely, *J. Am. Chem. Soc.* **116**, 11819 (1994).
- ²¹ S. Lee, M. M. Banaszak Holl, W. H. Hung, and F. R. McFeely, in *Modular Chemistry*, edited by J. Michl (Kluwer Academic, Dordrecht, The Netherlands, 1997), pp. 451–460.
- ²² K. Z. Zhang, M. M. Banaszak Holl, and F. R. McFeely, *Mater. Res. Soc. Symp. Proc.* **446**, 241 (1997).
- ²³ K. Z. Zhang, M. M. Banaszak Holl, and F. R. McFeely, *J. Phys. Chem.* **102**, 3930 (1998).
- ²⁴ K. Z. Zhang, J. N. Greeley, M. M. Banaszak Holl, and F. R. McFeely, *J. Appl. Phys.* **82**, 2298 (1997).
- ²⁵ K. Z. Zhang, L. M. Meeuwenberg, M. M. Banaszak Holl, and F. R. McFeely, *Jpn. J. Appl. Phys., Part 1* **36**, 1622 (1997).
- ²⁶ J. N. Greeley, L. M. Meeuwenberg, and M. M. Banaszak Holl, *J. Am. Chem. Soc.* **120**, 7777 (1998).
- ²⁷ K. T. Nicholson and M. M. Banaszak Holl, *Phys. Rev. B* **64**, 155317 (2001).
- ²⁸ K. S. Schneider, Z. Zhang, M. M. Banaszak Holl, B. G. Orr, and U. C. Pernisz, *Phys. Rev. Lett.* **85**, 602 (2000).
- ²⁹ Y. J. Chabal, *Surf. Sci. Rep.* **8**, 211 (1988).
- ³⁰ T. Hattori, *Crit. Rev. Solid State Mater. Sci.* **20**, 339 (1995).
- ³¹ J. N. Greeley, L. M. Meeuwenberg, and M. M. Banaszak Holl, *J. Am. Chem. Soc.* **120**, 7776 (1998).
- ³² W. Ehrley, R. Butz, and S. Mantl, *Surf. Sci.* **248**, 193 (1991).
- ³³ Y. Kobayashi and T. Ogino, *Surf. Sci.* **368**, 102 (1996).
- ³⁴ P. A. Agaskar, *Inorg. Chem.* **30**, 2707 (1991).
- ³⁵ P. Bornhauser and G. Calzaferri, *Spectrochim. Acta, Part A* **46**, 1045 (1990).
- ³⁶ M. D. Nyman, S. B. Desu, and C. H. Peng, *Chem. Mater.* **5**, 1636 (1993).
- ³⁷ C. Marcolli, P. Laine, R. Buhler, G. Calzaferri, and J. Thomkinson, *J. Phys. Chem. B* **101**, 1171 (1997).
- ³⁸ J. Eng *et al.*, *J. Chem. Phys.* **108**, 8680 (1998).
- ³⁹ S. Lee, S. M. M. M. Banaszak Holl, and F. R. McFeely, *J. Am. Chem. Soc.* **116**, 11819 (1994).

- ⁴⁰H. Z. Massoud, E. H. Poindexter, and C. R. Helms, *The Physics and Chemistry of SiO₂ and the Si-SiO₂ Interface* (The Electrochemical Society, Pennington, NJ, 1996), Vol. 3.
- ⁴¹K. Z. Zhang, M. M. Banaszak Holl, and F. R. McFeely, *Mater. Res. Soc. Symp. Proc.* **446**, 241 (1997).
- ⁴²K. Z. Zhang, J. N. Greeley, M. M. Banaszak Holl, and F. R. McFeely, *J. Appl. Phys.* **82**, 2298 (1997).
- ⁴³K. Z. Zhang, M. M. Banaszak Holl, and F. R. McFeely, *J. Phys. Chem. B* **102**, 3930 (1998).
- ⁴⁴K. Z. Zhang, K. E. Litz, M. M. Banaszak Holl, and F. R. McFeely, *Appl. Phys. Lett.* **72**, 46 (1998).
- ⁴⁵F. R. McFeely, K. Z. Zhang, M. M. Banaszak Holl, S. Lee, and J. E. Bender, *J. Vac. Sci. Technol. B* **14**, 2824 (1996).
- ⁴⁶A. B. Gurevich, M. K. Weldon, Y. J. Chabal, R. L. Opila, and J. Sapjeta, *Appl. Phys. Lett.* **74**, 1257 (1999).
- ⁴⁷J. W. Lyding, K. Hess, G. C. Abeln, D. S. Thompson, J. S. Moore, M. C. Hersam, E. T. Foley, J. Lee, Z. Chen, S. T. Hwang, H. Choi, Ph. Avouris, and I. C. Kizilyalli, *Appl. Surf. Sci.* **130–132**, 221 (1998).
- ⁴⁸J. W. Lyding, K. Hess, and I. C. Kizilyalli, *Appl. Phys. Lett.* **68**, 2526 (1996).